UDC 544.6.018.23+544.032.2

O.V. Boychuk [a], Ye.S. Pletenets [a], K.D. Pershina [a, b]

THERMOELECTRIC PROPERTIES OF THE MODIFIED NATURAL ALUMINOSILICATES

[a] V.I. Vernadsky Institute of General and Inorganic Chemistry of the National Academy of Sciences of Ukraine, Kyiv, Ukraine
[b] Joint Department of Electrochemical Energy Systems of the NAS of Ukraine, Kyiv, Ukraine

Natural layered bentonite and its artificial modifications have attracted growing interest in converting low-grade thermal energy into electricity. However, a substantial improvement in the thermoelectrical performance of modified clay remains a significant challenge. Modification is one way to solve the rising thermoelectrical efficiency of clays. Natural bentonite is a promising material for modifications by phosphate ions and magnetite because it is easily prepared in the water media. Such modifications demonstrated high thermoelectrical performance (increasing the Seebek coefficient by two times), thermostability, and durability. IR spectroscopy, X-ray diffraction analysis, atomic absorption spectroscopy, surface area measurements, SEM microscopy, and electrochemical impedance spectroscopy measurements have given the possibility to detect differences in the thermoelectric behavior of the natural and modified bentonite. Magnetite in bentonite enhances the Seebeck coefficient via localization of charge distribution and change in the size of pores, enlarging the non-linear distribution of the electrostatic capacitance due to changing the distribution of the absorbed water, surface, and structure's OH^- groups in the natural bentonite. The modification by magnetite decreases the size of the pores to $50-100$ nm in bentonite and increases the Seebeck coefficient by 30% on average. The incorporation of phosphate ions causes the decrease of the thermoelectric effect under rising the temperature. Design by PO_4^{3-} increases the pore sizes more than two times and drops the Seebeck coefficient by 70% on average.

Keywords: bentonite, thermoelectricity, porous size, phosphate ions, magnetite.

Introduction

The growing tendency to using low carbon energy fuels and adverse environmental impact of fossil fuel are associated with new solution and urgent need for alternative energy sources. Thermoelectricity may be one of the key solutions to make energy production more sustainable owing to the natural heat gradients generated by natural sources (sun, thermal waters etc.) and by the industrial activity of the people. Today, a wide range of new thermoelectric materials have been proposed and studied, technologies for their production have been developed, and devices for converting heat into electricity are available. Despite the potential advantages, the currently available options for heat recovery, such as Bi_2Te_3-based thermoelectric modules, are hampered by high costs, limiting their widespread application [1]. Moreover, many materials with potentially high energy conversion efficiency have metastable compositions, leading to a lack of durability and reliability in practical applications. As a result, it is needed to develop a new generation of thermoelectric materials that would be cost-effective, highly efficient for energy recovery and stable, to

unlock the full potential of thermoelectric technology for low-grade heat transformation.

The abundance of natural aluminosilicate-based materials with thermoelectric properties makes them a compelling alternative for ambient energy harvesting. Natural and modified clay minerals are widely used in industry and environmental protection, especially as adsorbents, molecular sieves, ion exchange materials, and catalysts [2]. In addition, these minerals are the starting material for the synthesis of columnar clays and porous clay heterostructures, which are used as a matrix for creating composites with thermoelectric properties [3–5].

The origin of the thermoelectric effect in cement pastes containing steel fibers was analyzed in works [6,7]. The existence of a positive charge in the bulk of the paste due to the formation of a p-n heterojunction at the aluminosilicate matrix-metal fiber interface was determined. It was also established that ion transport is caused by the presence of water contained inside the pores and contributes to the appearance of the thermoelectric effect and the formation of ion conductivity [8,9]. An additional influencing factor is temperature, which creates conditions for water loss, which reduces the share of ionic conductivity and increases electronic conductivity [9]. Cai et al. [10] analyzed the influence of the concentration of alkali and carbon impurities (ash) on the realization and value of the Seebeck effect in layered aluminosilicates based on metakaolin and Portland cement. Increasing the alkali concentration increased the density of samples, contributing to the formation of electron transport. This led to higher values of thermoelectric coefficients than in reference samples based on Portland cement. The same effect was shown by the aluminosilicates modified by phosphoric acid. To increase the voltage that occurs due to the thermal effect in thermoelectrics, it is proposed to use composite materials in which layered aluminosilicates and their modified forms are a matrix, to which, in order to increase the internal temperature, metal nanoparticles, graphene, carbon nanotubes and two-dimensional carbides of transition metals are added. These materials, due to the accumulation of additional heat, create micro-areas with tension over the entire surface of the matrix. Such materials with certain additives, and even alone under certain conditions, can work as thermoelectrics or piezoelectrics.

In the case of acidic modifications, after heat treatment, a decrease in the dielectric constant of materials and an increase in their conductivity are observed [11,12]. According to these properties of the composites with alumosilicates the target of this study was to compare the physico-chemical and thermoelectric properties of natural clay, clay modified by phosphoric ions and composite material with natural clay and mixture of iron oxides (Fe_3O_4).

Materials and methods

The natural bentonite came from Dashuki, Ukraine (Table 1). Phosphate-ion modification of bentonite was done at low temperature in a 1 M aqueous solution of phosphoric acid (H_3PO_4) for 3 hours with further treatment with water and drying in open air.

The modification of natural bentonite with Fe_3O_4 had the following steps: (1) 10 g of natural bentonite was added to 10 ml of 1 mol/dm^3 aqueous solution of $FeCl_3$; (2) the resulting suspension was stirred for 30 minutes to obtain a stable water suspension of clay; and (3) 25% aqueous solution of NH_3 was added dropwise to achieve pH 9. The resulting product was washed with distilled water to a pH of 8 and dried at room temperature for 7 days.

The spectra were recorded using a Nicolet Nexus 470 spectrometer. The IR spectra of attenuated total internal reflection (attenuated total reflection, ATR) were recorded for ground powdered samples, without sample preparation and dilution, using a PPVV Smart Orbit attachment (manufactured by Thermo Scientific), a diamond was the optical element. The angle of the incident beam $\theta=45^0$. The wave range was $4000–400$ cm^{-1}, the number of scans was 128, and the resolution was 4 cm^{-1}. The background was recorded relative to the optical element without the sample.

Mineralogical analyses were performed through X-ray diffraction (XRD) using a DRON-4-07 diffractometer equipped with a copper tube (λ $CuK_{\alpha mean}=1.5418$ Е, λ $CuK_{\alpha1}=1.54060$ Е, and λ $CuK_{\alpha2}=1.54439$ Е). The measurement was conducted under the following conditions: 40 kV and 40 mA, with a 2theta sweep ranging from 5 to 60 degrees, with a shooting step of 0.05^0 and an exposure time of 3 s. The database of the International Committee for Powder Diffraction Data (ICDD) and the Match computer program developed by Dr. K. Brandenburg & Dr. H. Putz GbR (Germany) were used to indicate the phase composition of the samples.

The contents of metals were evaluated by the use of flame atomic absorption spectrometry. A High-Resolution Continuum Source Atomic Absorption Spectrometer Philips SP09 with a 300 W xenon short-arc lamp as a continuum radiation source was applied. Acetylene was used as the fuel, while the oxidant

O.V. Boychuk, Ye.S. Pletenets, K.D. Pershina

Table 1

Composition and structure of samples

Sample	Macroelement content, wt.%	Structure
Bentonite	SiO_2 68.64 Al_2O_3 11.50 TiO_2 0.32 Fe_2O_3 1.56 CaO 1.46 MgO 0.50 Na_2O 2.34 K_2O 2.40	Lamellar The size of grains is 50–110 nm
Bentonite modified by phosphate ions	SiO_2 68.64 Al_2O_3 11.50 TiO_2 0.32 Fe_2O_3 1.56 CaO 1.46 MgO 0.50 Na_2O 2.34 K_2O 2.40 P_2O_5 up to 5	Lamellar The size of grains is 50–70 nm
Bentonite modified by iron oxides	SiO_2 68.64 Al_2O_3 11.50 TiO_2 0.32 Fe_3O_4 4.38 CaO 1.46 MgO 0.50 Na_2O 2.34 K_2O 2.40	Mixture of lamellar and rolled conglomerates The size of grains is 50–800 μm

was air. The measurements were performed at 248.327 nm (Fe), 365.482 nm (Ti), 421.725 nm (Ca), 284.725 nm (Mg), 766.321 (K), and 589.347 (Na). The measurements were performed eleven times for each sample. Quantification was based on a calibration curve (r=0.9999) estimated for each standard solution.

The specific surface area was calculated by the BET method using an Automatic Sorption Analyzer Porosimetry system 2020 comprising a pressure transducer (Micromeritics, Norcross, GA, USA). The sorbent samples were outgassed on the degas port of the analyzer at 250^0C for 12 h. The sorption isotherms were created by adding nitrogen to the sorbent at 77 K.

The impedance spectra and open circuit potential (OCP) of the samples were recorded in a two-electrode cell on an Autolab 30 PGSTAT301N Metrohm Autolab electrochemical module in a two-electrode cell (disk cell) with Cu contacts equipped with a FRA (Frequency Response Analyzer) module in the frequency range $10^{-2}-10^6$ Hz. An electromechanical thermostat with an accuracy of temperature of $\pm1^0C$ was used to ensure the necessary

temperature interval. The results were processed using Nova 2.1 and ZView2 software.

Electrical conductivity was calculated from impedance data by the equation:

$$\sigma = \frac{1}{Z'}, \tag{1}$$

where Z' as the active resistance of the sample.

The open-circuit voltage of the samples was measured using a homemade experimental setup (Fig. 1).

The tablets with a diameter of 16 mm for Seebeck behavior measurements were prepared from dry powder samples under the pressure of 2 MPa.

The calculation of the Seebeck Coefficient was done according to the following equation:

$$S_{coeff} = \frac{OCP_{T_2} - OCP_{T_1}}{T_2 - T_1}, \tag{2}$$

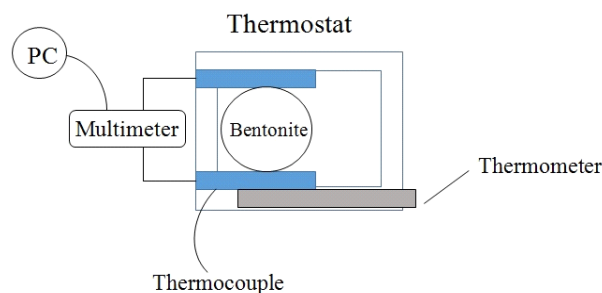where OCP is the open circuit potential (mV), T_1 is the starting temperature (K), and T_2 is the ending

Fig. 1. Schematic diagram of the experimental setup for the measurement of thermoelectric behavior

Fig. 3. X-ray diffraction patterns of bentonite in the range $2\theta=5-10^0$: 1 − natural bentonite; and 2 − bentonite with magnetite

temperature (K).

The SEM images of the sample surfaces were obtained with a scanning electron microscope (TESCAN VEGA 3) with Bruker Company software.

Results and discussions

Bentonite and modified bentonite used in this study were characterized using X-ray diffraction, atomic absorption spectroscopy, IR spectroscopy and SEM to determine their chemical composition, crystalline phases, structure and surface changes. The chemical analysis of samples of natural bentonite and bentonite modified by phosphate ions did not show any difference in the amount of metal ions (Table 1). The same results were obtained for the crystalline phase amount and composition of these samples. A set of peaks are superimposed on the main background, corresponding to a complex mixture of crystalline phases, including montmorillonite (M); quartz (Q), SiO_2; cristobalite (C), SiO_2; and magnetite (F), Fe_3O_4. So, the modification by phosphate ions didn't affect the composition, nature and amount of phases in the natural bentonite. The modification of magnetite changed the amount of iron in bentonite and
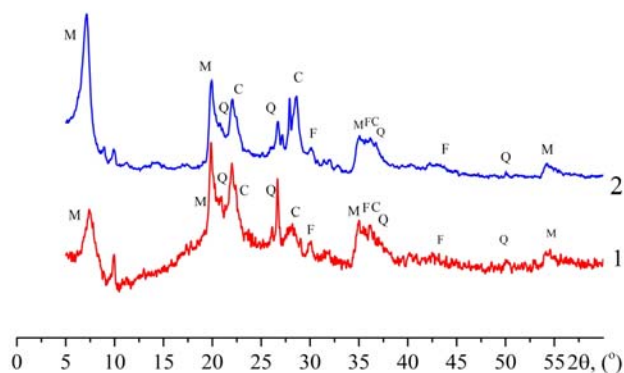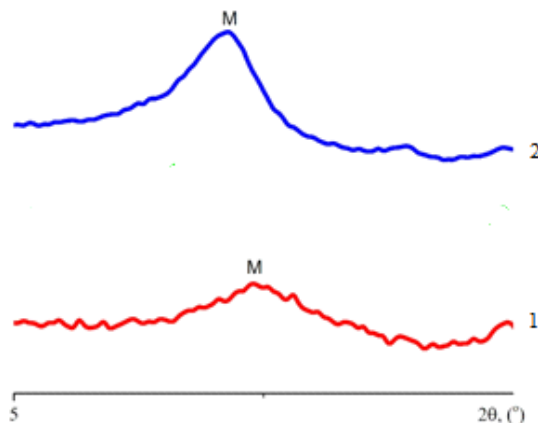
increased the intensity (value) of montmorillonite in a small angle range (Figs. 2 and 3).

IR spectroscopy detected the main differences in the impact of modification. In the case of modification by phosphate ions, the main changes occurred in the following regions: $3700-3621$ cm^{-1} OH^{-} (structure groups with n type of oscillations); $3400-3396$ cm^{-1}, H_2O (ads.) with ν type of oscillations; 1650 cm^{-1}, H_2O (ads.) with δ type of oscillations; and 987 cm^{-1}, OH^{-} (surface groups with δ type of oscillations). Fe(III)$-$O in octahedral position with δ type of oscillations was not detected ($470-430$ cm^{-1}) after PO_4^{3-} modification (Figs. 4 and 5).

The IR spectrum of bentonite with Fe_3O_4 showed the full disappearance of H_2O (ads.), with ν type of oscillations in the $3400-3396$ cm^{-1} region and a great decrease of the OH^{-} structure groups with ν type of oscillations in the $3700-3621$ cm^{-1} range; H_2O (ads.) with δ type of oscillations in the

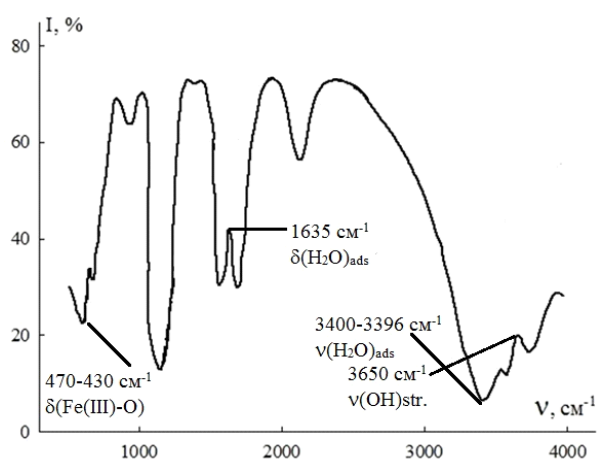Fig. 2. X-ray diffraction patterns of bentonite in the range $2\theta=5-60^0$: 1 − bentonite with magnetite; and 2 − natural bentonite. Conventional designations: M − montmorillonite; Q − SiO_2 (quartz); C − SiO_2 (cristobalite); and F − Fe_3O_4 (magnetite)

Fig. 4. IR spectrum of natural bentonite

O.V. Boychuk, Ye.S. Pletenets, K.D. Pershina
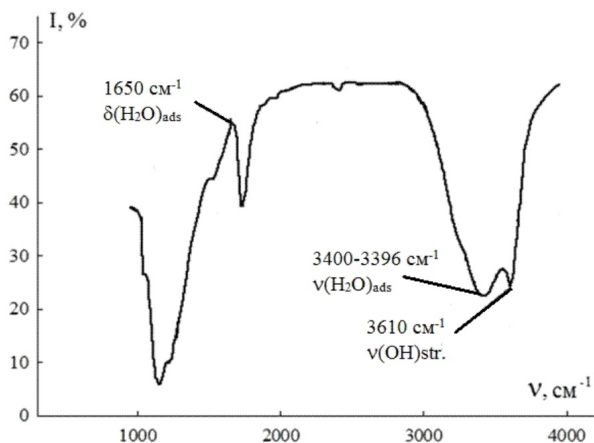
Fig. 5. IR spectrum of natural bentonite modified by phosphate ions

Fig. 7. SEM image of natural bentonite

1650 cm^{-1} region of the spectrum. The small reflexes in the 1575 cm^{-1} region may be accorded to OH-groups with δ type of oscillations. In addition, mixed Si$-$O$-$Al and Mg$-$O with δ type of oscillations were well recognized. Fe(III)$-$O in octahedral position with δ type of oscillations is fully saved in the $470-430$ cm^{-1} region (Fig. 6). Thus, the modification by magnetite changes the distribution of the absorbed water and surface and structure OH$^-$ groups in the own structure of bentonite. Modification by phosphate ions decreases the amount of the iron oxides.

SEM and the porometric study of materials detected the main impact of modification on surface morphology. Modification by PO$_4^{3-}$ ions increases the surface area and changes the ratio of the pore sizes relative to natural bentonite (Figs. 7 and 8). Two kinds of pores (micro- and mezo-) have been detected in these samples (Table 2).
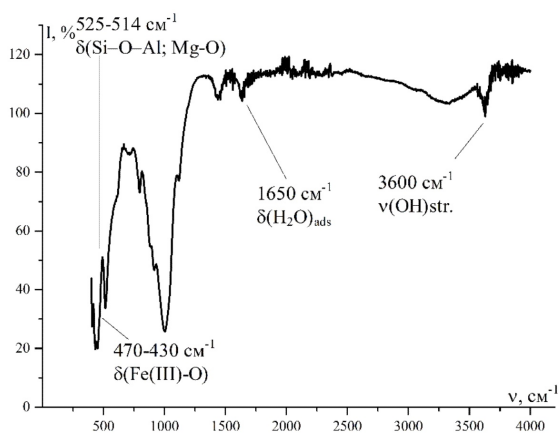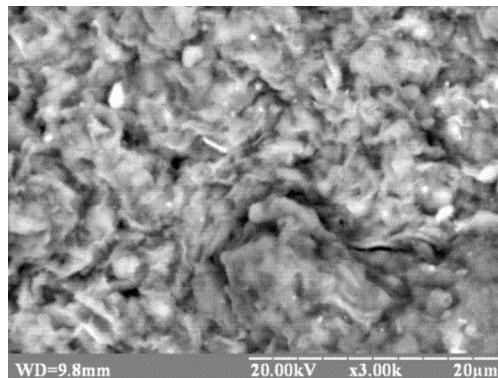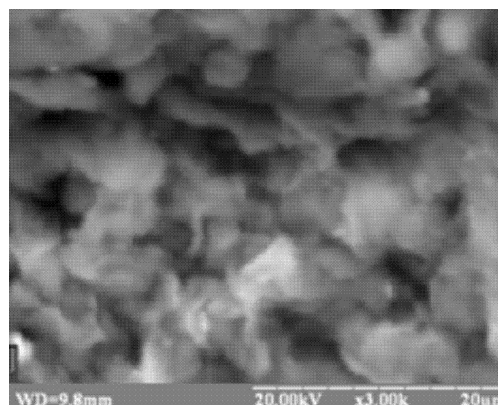

Fig. 8. SEM image of bentonite modified by phosphate ions

Table 2

Surface area and pore size of natural bentonite, bentonite modified by phosphate ions and bentonite modified by Fe$_3$O$_4$

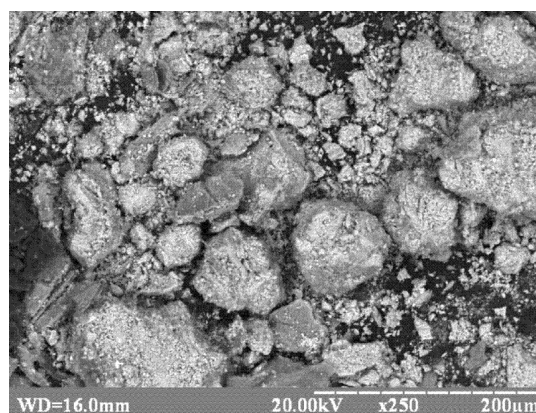| Sample	$S_{surface}$, m^2/g	Pore size, nm
natural bentonite	36	150–200
bentonite modified by phosphate ions	72	70–200
bentonite modified by Fe$_3$O$_4$	18	50–100

Fig. 6. IR spectrum of bentonite with magnetite

Fig. 9. SEM image of bentonite modified by Fe$_3$O$_4$

The addition of magnetite affects the growth of conglomerates up to 800 μm on the surface (Fig. 9) which decreases the surface area and pore size (Table 2). Most of pores have a micro-size (50−70 nm). Most of aluminosilicate pores have a micro-size (50−70 nm). In addition, magnetite has own phase as a component of mixture.

To evaluate the impact of temperature on electrical conductivity, an impedance spectroscopy test of three parallel samples (Table 3) was conducted at two temperatures (20°C and 40°C) in the frequency range of 10^{-1} to 10^6 Hz. The samples of natural bentonite have similar dependence of change in electrical conductivity at 20°C and 40°C with decreasing ionic conductivity [13,14]. Conductivity increase correlates with changing the sample weight at 20°C. At 40°C, this correlation is lost (Fig 10,a,b). Such behavior may be associated with disordered desorption of adsorbed water during temperature rise.

The specific electrical conductivity value of bentonite modified by phosphate ions is an order of magnitude lower than the conductivity of natural bentonite, but the common trend of its change in the same frequency range is similar (Fig. 11).

Table 3

Weight of samples of natural bentonite and modified bentonite

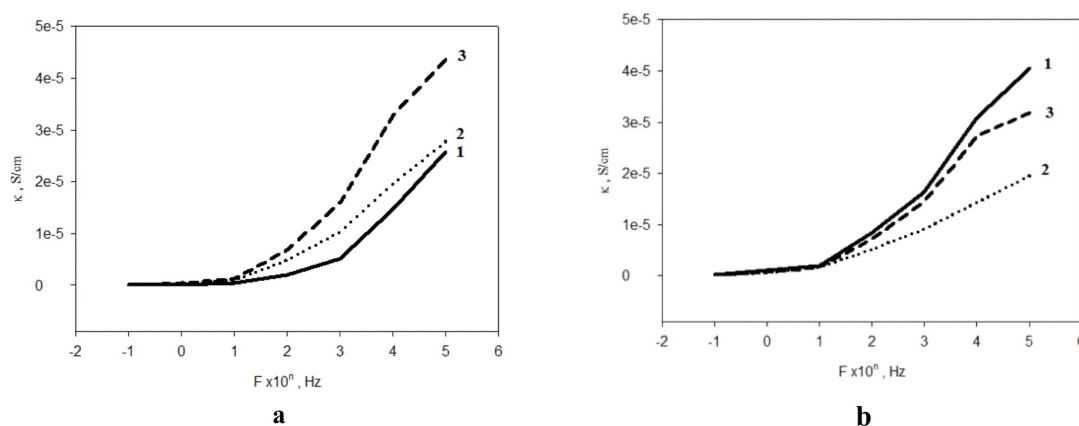| Sample	Weight, g		
	No. 1	No. 2	No. 3
natural bentonite	1.4075±0.0085	1.4080±0.0085	1.4100±0.0085
bentonite modified by phosphate ions	1.4490±0.004	1.4625±0.004	1.4645±0.004
bentonite modified by Fe_3O_4	1.4120±0.003667	1.4435±0.003667	1.4155±0.003667

Fig. 10. Dependence of specific electrical conductivity in natural bentonite on frequency: (a) at 20°C; and (b) at 40°C
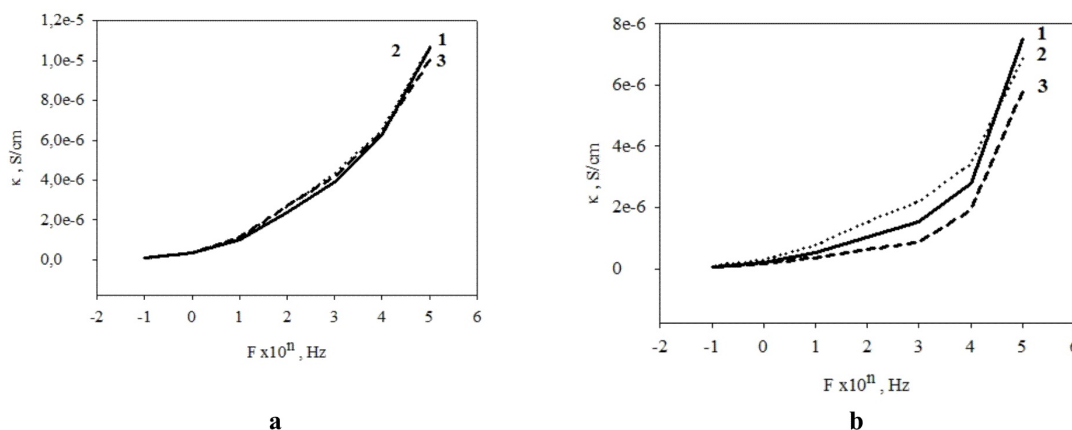

Fig. 11. Dependence of specific electrical conductivity in bentonite modified by phosphate ions on frequency: (a) at 20°C; and (b) at 40°C
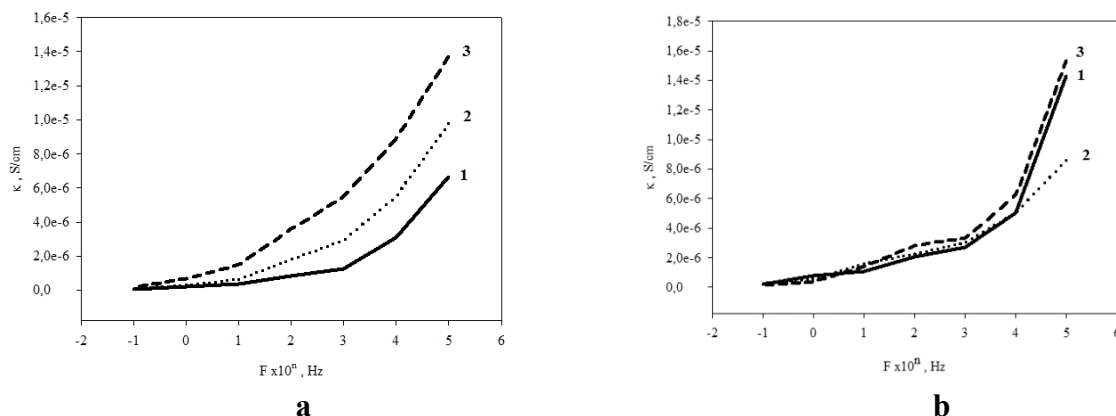
O.V. Boychuk, Ye.S. Pletenets, K.D. Pershina

Fig. 12. Dependence of specific electrical conductivity in bentonite modified by Fe_3O_4 on frequency: (a) at 20^0C; and (b) at 40^0C

The samples of bentonite modified by Fe_3O_4 have a little bit lower specific electrical conductivity than natural bentonite with the same tendency of change (Fig. 12).

The conductivity value of all samples of natural and modified bentonite indicates the presence of ionic conductivity because they have the maximum conductivity in the high frequency range (10^5 Hz). However, the change in OCP does not show any dependence on conductivity value in the low frequency region.

Further comparison of the active resistance (Z') as a function of conductivity, and dispersion of the electrostatic capacity ($C\omega$) in the high frequency range (10^5 Hz) indicated zones with non-homogeneous capacity dispersion in the case of an increase in OCP (Figs. 13−15):

$$C(\omega) = 1/[Z_\omega - Z_{\omega\to\infty}]i\omega, \qquad (3)$$

where Z_ω is the impedance data at the current frequency; ω is the frequency; and i is the electric current density.

The temperature impact leads to the appearance of regions with a non-linear dependence of voltage, capacitance and resistance and to the formation of local layers with different values of dielectric permeability and ion diffusion rate [15]:

$$Z_{(S)} = R_w w_d^{1-\gamma}(w_d/s)^{\gamma/2} \coth[s/w_d^{1-\gamma/2}], \qquad (4)$$

$$R_w = Z'_\omega, \quad R_\omega = \frac{L}{qAD}\left(\frac{dE}{dc}\right), \qquad (5)$$

where L is the thickness of the diffusion layer (0>x>L); A is the surface area of the electrode; D is the diffusion coefficient; q is the charge passing through the surface; dc is the change in ion concentration; dE is the potential difference in the layer of thickness L; and s is the Laplace variable assigned to the angular frequency ω at $s=i\omega$, $\omega=2\pi f$ (here f is the alternating current frequency and γ is the exponential coefficient).

According to these equations, it became possible to assign the dispersion of capacity as a function of charge distribution on the surface, which could takes place in the presence of some compounds or groups in bentonite.

The presence of magnetite decreases the size of pores in bentonite and increases the Seebeck coefficient, the maximum value of this coefficient being observed in the sample with minimum size of pores. Modification by PO_4^{3-} ions shows an opposite tendency. It increases the pore size and decreases the Seebeck coefficient. Moreover, OCP decreases with decreasing the temperature in these samples (Table 4, Figs. 13−15).

Table 4

Seebeck coefficient and pore size of natural bentonite and modified bentonite

| No.	Samples	Size of pores, nm	Seebeck coefficient, mV/K
1	natural bentonite	150–170	3.0±0.02
2	natural bentonite	150–200	1.3±0.02
3	natural bentonite	150–160	4.1±0.02
1	bentonite with PO_4^{3-} ions	200–250	1.4±0.02
2	bentonite with PO_4^{3-} ions	200–250	1.2±0.02
3	bentonite with PO_4^{3-} ions	200–250	1.2±0.02
1	bentonite with Fe_3O_4	50–100	3.4±0.02
2	bentonite with Fe_3O_4	50–60	4.8±0.02
3	bentonite with Fe_3O_4	50–70	4.1±0.02
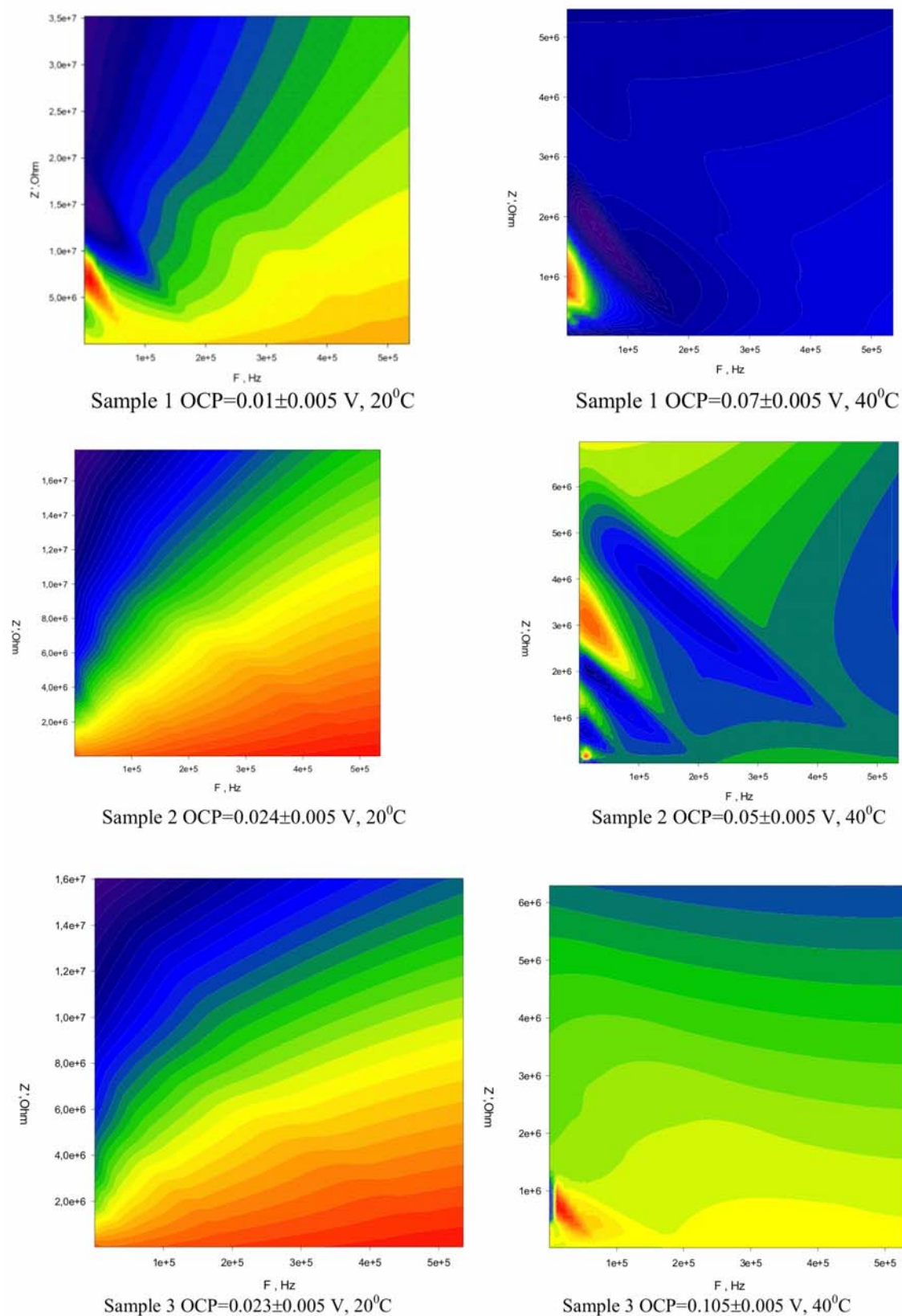
Fig. 13. Correlation of the active resistance (Z') and electrostatic capacity dispersion (C_d) with the frequency in the samples of the natural bentonite at 20^0C and 40^0C

O.V. Boychuk, Ye.S. Pletenets, K.D. Pershina

Fig. 14. Correlation of the active resistance (Z') and electrostatic capacity dispersion (C_d) with the frequency in samples of bentonite modified by phosphate ions at 20^0C and 40^0C
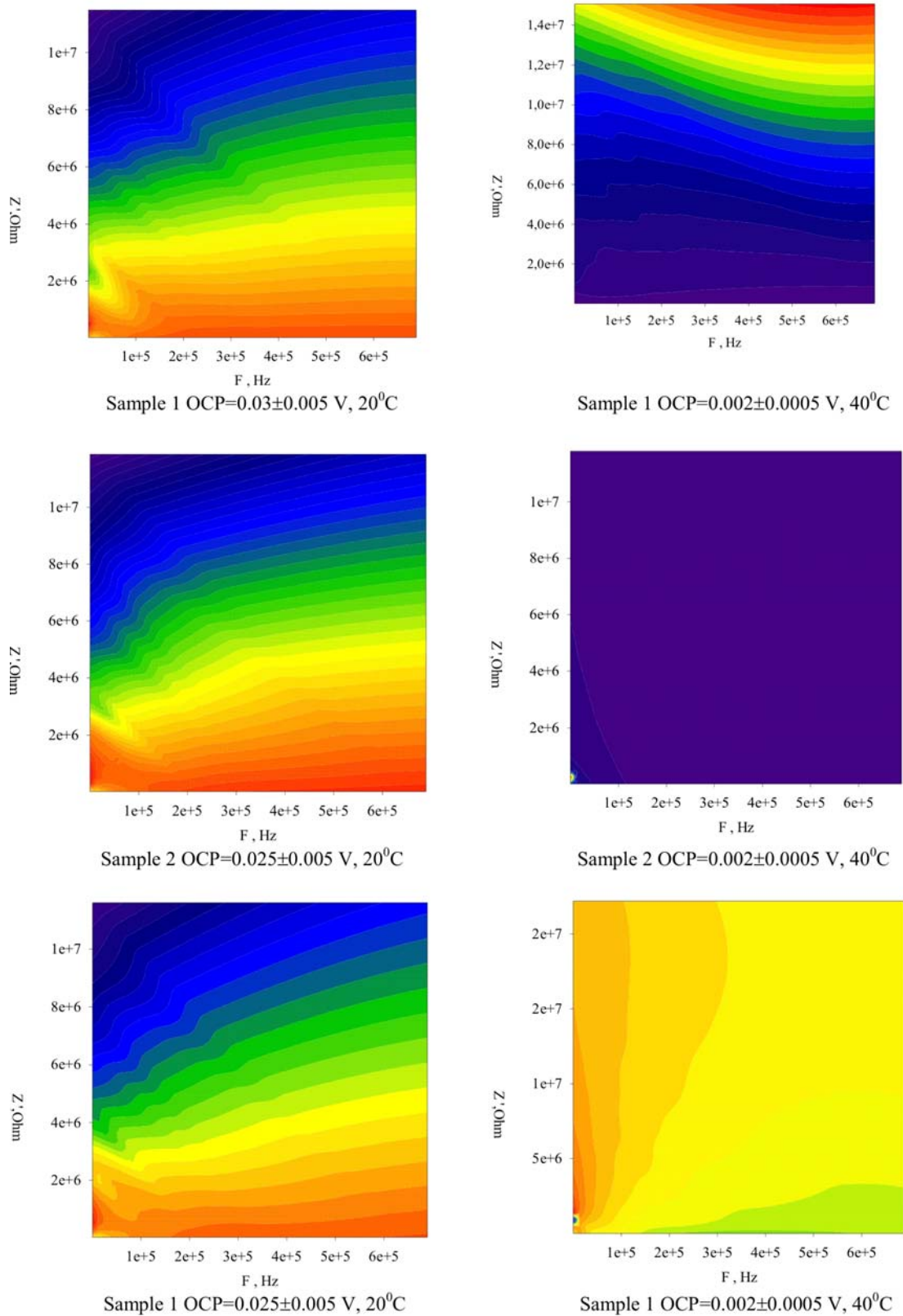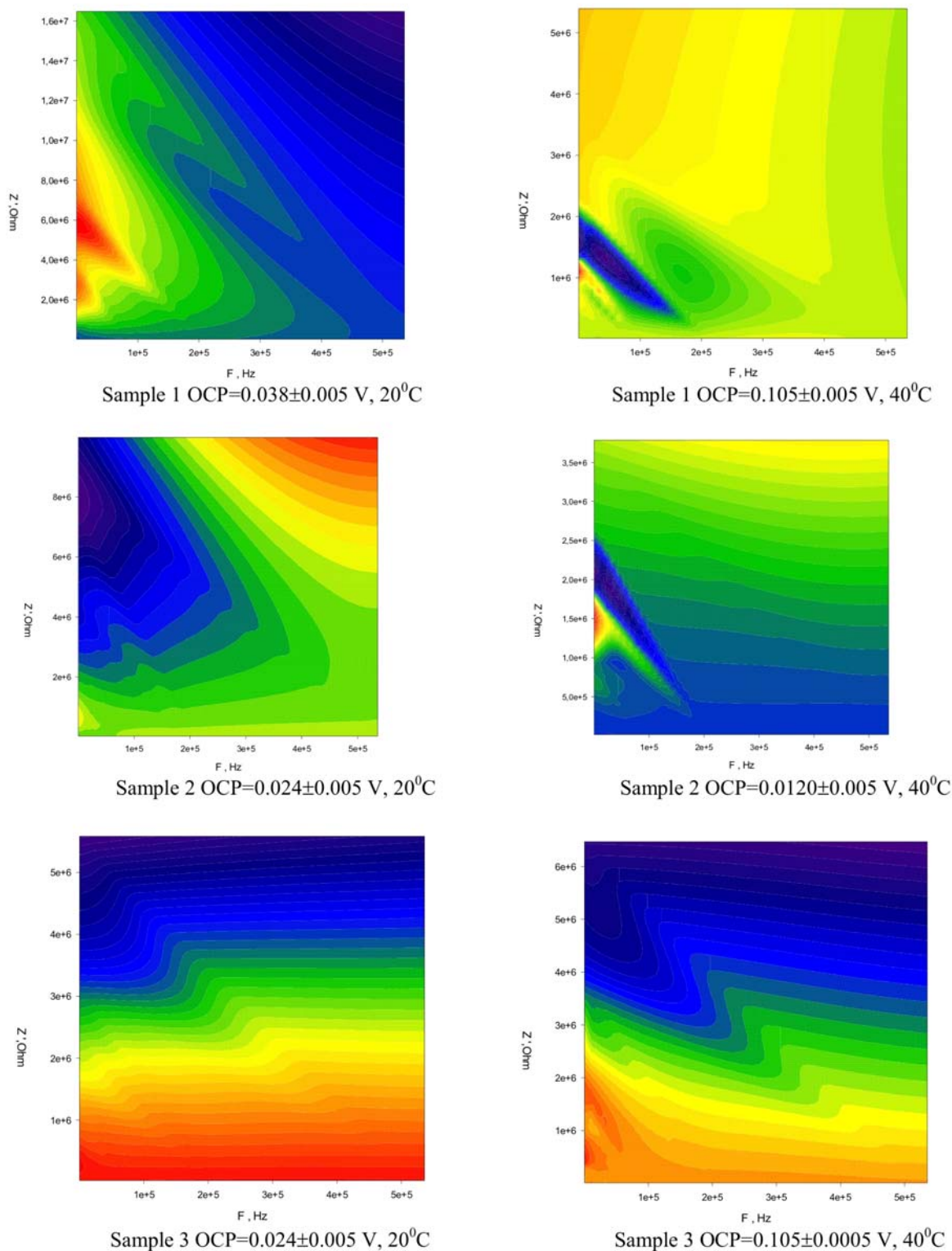
Fig. 15. Correlation of the active resistance (Z') and electrostatic capacity dispersion (C_d) with the frequency in samples of bentonite modified by Fe_3O_4 at 20^0C and 40^0C

Conclusions

Natural bentonite has good thermoelectric properties with Seebeck coefficient of 1.4 to 4.1 mV/K. The modification of natural bentonite can be used to change its thermoelectric properties using functional additives affecting electrostatic capacity dispersion connected with charge distribution. Additives are the main factor to affect the pore size and thermoelectric effectiveness of the material through changing the kind of adsorbed water and structural surface OH groups. Modification by magnetite decreases the size of pores in bentonite and increases the Seebeck coefficient value by 30% on average. The presence of PO_4^{3-} ions increases the pore size, and decreases the Seebeck coefficient by 70% on average during heating. The study provides insight into new prospects for enhancing the thermoelectric performance of natural clay and its modified forms for thermoelectric energy harvesting in a narrow temperature range.

REFERENCES

1. *Performance* of Bi_2Te_3-based thermoelectric modules tailored by diffusion barriers / Nguyen Y.N., Kim K.T., Chung S.H., Son I. // J. Alloys Compd. − 2022. − Vol.895. − Art. No. 162716.

2. *General* introduction: clays, clay minerals, and clay science / Bergaya F., Lagaly G. // Develop. Clay Sci. − 2006. − Vol.1. − P.1-18.

3. *High* performance Bi_2Te_3 nanocomposites prepared by single-element-melt-spinning spark-plasma sintering / Xie W., Wang S., Zhu S., He J., Tang X., Zhang Q., Tritt T.M. // J. Mater. Sci. − 2013. − Vol.48. − No. 7. − P.2745-2760.

4. *Complex* thermoelectric materials / Synder G.J., Toberer E.S. // Nat. Mater. − 2008. − Vol.7. − P.105-114.

5. *Thermoelectric* figure of merit of a one-dimensional conductor / Hicks L.D., Dresselhaus M.S. // *Phys. Rev. B.* − 1993. − Vol.47. − No. 24. − P.16631-16634.

6. *Origin* of the thermo-electric behavior of steel fiber cement paste / Wen S., Chung D.D.L. // Cem. Concr. Res. − 2002. − Vol.32. − No. 5. − P.821-823.

7. *Effect* of fiber content on the thermoelectric behavior of cement / Wen S., Chung D.D.L. // J. Mater. Sci. − 2004. − Vol.39. − No. 13. − P.4103-4106.

8. *Piezoelectric* effect of hardened cement paste / Sun M., Li Z., Song X. // Cem. Concr. Compos. − 2004. − Vol.26. − No. 6. − P.717-720.

9. *Role* of moisture in the Seebeck effect in cement-based materials / Cao J., Chung D.D.L. // Cem. Concr. Res. − 2005. − Vol.35. − No. 4. − P.810-812.

10. *Thermoelectric* behaviors of fly ash and metakaolin based geopolymer / Cai J., Tan J., Li X. // Constr. Build. Mater. − 2020. − Vol.237. − Art. No. 117757.

11. *A novel* aluminosilicate geopolymer material with low dielectric loss / Cui X.M., Liu L.P., He Y., Chen J.Y., Zhou J. // Mater. Chem. Phys. − 2011. − Vol.130. − No. 1-2. − P.1-4.

12. *Enhanced* dielectric performance of metakaolin−H_3PO_4 geopolymers / Douiri H., Louati S., Baklouti S., Arous M., Fakhfakh Z. // Mater. Lett. − 2016. − Vol.164. − P.299-302.

13. *Electrochemical* properties of sodium bis [salicylato (2-)]-borate-γ-butyrolactone electrolytes in sodium battery / Diamant V.A., Malovanyy S.M., Pershina K.D., Kazdobin K.A. // Mater. Today Proc. − 2019. − Vol.6. − P.86-94.

14. *Electrochemical* impedance spectroscopy / Orazem M.E., Tribollet B. // New Jersey. − 2008. − Vol.1. − P.383-389.

15. *Control* of the state of primary alkaline Zn−MnO_2 cells using the electrochemical impedance spectroscopy method / Riabokin O.L., Boichuk A.V., Pershina K.D. // Surf. Eng. Appl. Electrochem. − 2018. − Vol.54. − P.614-622.

ТЕРМОЕЛЕКТРИЧНІ ВЛАСТИВОСТІ МОДИФІКОВАНИХ ПРИРОДНИХ АЛЮМОСИЛІКАТІВ

О.В. Бойчук, Є.С. Плетенець, К.Д. Першина

Природний шаруватий бентоніт та його штучні модифікації викликають зростаючий інтерес у зв'язку перетворенням низькопотенційної теплової енергії в електричну. Однак суттєве покращення термоелектричних характеристик модифікованої глини залишається серйозною проблемою. Модифікація є одним із способів вирішення проблеми підвищення термоелектричної ефективності глин. Природний бентоніт є перспективним матеріалом для модифікації фосфат-іонами та магнетитом, оскільки легко готується у водному середовищі. Такі модифікації продемонстрували високі термоелектричні характеристики (збільшення коефіцієнта Зеєбека вдвічі), термостабільність і довговічність. ІЧ-спектроскопія, рентгенівський дифракційний аналіз, атомно-абсорбційна спектроскопія, вимірювання площі поверхні, СЕМ-мікроскопія та вимірювання спектроскопії електрохімічного імпедансу дали можливість виявити відмінності в термоелектричній поведінці природного та модифікованого бентоніту. Магнетит у бентоніті підвищує коефіцієнт Зеєбека за рахунок локалізації розподілу заряду та зміни розміру пор, збільшуючи нелінійний розподіл електростатичної ємності через зміну розподілу поглиненої води, поверхні та структурних ОН⁻ груп у природному бентоніті. Модифікація магнетитом зменшує розмір пор до 50−100 нм у бентоніті та збільшує середнє значення коефіцієнта Зеєбека на 30%. Включення фосфат-іонів викликає зниження термоелектричного ефекту при підвищенні температури. Дизайн PO_4^{3-} збільшує розміри пор більш ніж у два рази та знижує коефіцієнт Зеєбека в середньому на 70%.

Ключові слова: бентоніт, термоелектрика, пористість, фосфат-іони, магнетит.

THERMOELECTRIC PROPERTIES OF THE MODIFIED NATURAL ALUMINOSILICATES

*O.V. Boychuk [a], Ye.S. Pletenets [a], K.D. Pershina [a, b, *]*

[a] **V.I. Vernadsky Institute of General and Inorganic Chemistry of the National Academy of Sciences of Ukraine, Kyiv, Ukraine**

[b] **Joint Department of Electrochemical Energy Systems of the NAS of Ukraine, Kyiv, Ukraine**

[*] **e-mail: Pershina@ionc.kiev.ua**

Natural layered bentonite and its artificial modifications have attracted growing interest in converting low-grade thermal energy into electricity. However, a substantial improvement in the thermoelectrical performance of modified clay remains a significant challenge. Modification is one way to solve the rising thermoelectrical efficiency of clays. Natural bentonite is a promising material for modifications by phosphate ions and magnetite because it is easily prepared in the water media. Such modifications demonstrated high thermoelectrical performance (increasing the Seebek coefficient by two times), thermostability, and durability. IR spectroscopy, X-ray diffraction analysis, atomic absorption spectroscopy, surface area measurements, SEM microscopy, and electrochemical impedance spectroscopy measurements have given the possibility to detect differences in the thermoelectric behavior of the natural and modified bentonite. Magnetite in bentonite enhances the Seebeck coefficient via localization of charge distribution and change in the size of pores, enlarging the non-linear distribution of the electrostatic capacitance due to changing the distribution of the absorbed water, surface, and structure's OH^- groups in the natural bentonite. The modification by magnetite decreases the size of the pores to $50-100$ nm in bentonite and increases the Seebeck coefficient by 30% on average. The incorporation of phosphate ions causes the decrease of the thermoelectric effect under rising the temperature. Design by PO_4^{3-} increases the pore sizes more than two times and drops the Seebeck coefficient by 70% on average.

Keywords: bentonite; thermoelectricity; porous size; phosphate ions; magnetite.

REFERENCES

1. Nguyen YN, Kim KT, Chung SH, Son I. Performance of Bi_2Te_3-based thermoelectric modules tailored by diffusion barriers. *J Alloys Compd.* 2022; 895: 162716. doi: 10.1016/j.jallcom.2021.162716.

2. Bergaya F, Lagaly G. General introduction: clays, clay minerals, and clay science. *Dev Clay Sci.* 2006; 1: 1-18. doi: 10.1016/S1572-4352(05)01001-9.

3. Xie W, Wang S, Zhu S, He J, Tang X, Zhang Q, et al. High performance Bi_2Te_3 nanocomposites prepared by single-element-melt-spinning spark-plasma sintering. *J Mater Sci.* 2013; 48: 2745-2760. doi: 10.1007/s10853-012-6895-z.

4. Synder GJ, Toberer ES. Complex thermoelectric materials. *Nat Mater.* 2008; 7: 105-114. doi: 10.1038/nmat2090.

5. Hicks LD, Dresselhaus MS. Thermoelectric figure of merit of a one-dimensional conductor. *Phys Rev B.* 1993; 47: 16631-16634. doi: 10.1103/PhysRevB.47.16631.

6. Wen S, Chung DDL. Origin of the thermo-electric behavior of steel fiber cement paste. *Cem Concr Res.* 2002; 32: 821-823. doi: 10.1016/S0008-8846(01)00754-2.

7. Wen S, Chung DDL. Effect of fiber content on the thermoelectric behavior of cement. *J Mater Sci.* 2004; 39: 4103-4106. doi: 10.1023/B:JMSC.0000033389.83459.8f.

8. Sun M, Li Z, Song X. Piezoelectric effect of hardened cement paste. *Cem Concr Compos.* 2004; 26: 717-720. doi: 10.1016/S0958-9465(03)00104-5.

9. Cao J, Chung DDL. Role of moisture in the Seebeck effect in cement-based materials. *Cem Concr Res.* 2005; 35: 810-812. doi: 10.1016/j.cemconres.2004.05.036.

10. Cai J, Tan J, Li X. Thermoelectric behaviors of fly ash and metakaolin based geopolymer. *Constr Build Mater.* 2020; 237: 117757. doi: 10.1016/j.conbuildmat.2019.117757.

11. Cui XM, Liu LP, He Y, Chen JY, Zhou J. A novel aluminosilicate geopolymer material with low dielectric loss. *Mater Chem Phys.* 2011; 130: 1-4. doi: 10.1016/j.matchemphys.2011.06.039.

12. Douiri H, Louati S, Baklouti S, Arous M, Fakhfakh Z. Enhanced dielectric performance of metakaolin$-H_3PO_4$ geopolymers. *Mater Lett.* 2016; 164: 299-302. doi: 10.1016/j.matlet.2015.10.172.

13. Diamant VA, Malovanyy SM, Pershina KD, Kazdobin KA. Electrochemical properties of Sodium bis[salicylato (2-)]-borate- γ-butyrolactone electrolytes in sodium battery. *Mater Today Proc.* 2019; 6: 86-94. doi: 10.1016/j.matpr.2018.10.079.

14. Orazem ME, Tribollet B. *Electrochemical impedance spectroscopy.* New Jersey: John Wiley & Sons, Inc.; 2008. doi: 10.1002/9780470381588.

15. Riabokin OL, Boichuk AV, Pershina KD. Control of the state of primary alkaline $Zn-MnO_2$ cells using the electrochemical impedance spectroscopy method. *Surf Eng Appl Electrochem.* 2018; 54: 614-622. doi: 10.3103/S1068375518060108.